

Chapter 10 ONE-DIMENSIONAL MODELS OF THE UPPER OCEAN

P. P. Niiler and E. B. Kraus

10.1 Introduction

The present paper has profited from many presentations and discussions by members of the "one-dimensional working group" in Urbino. These contributors were too numerous for active participation in the writing; their names are marked by asterisks in the text.

One-dimensional models of the upper ocean can be useful because bulk temperatures or salinities tend to vary more along a vertical distance of a hundred meters than along a horizontal distance of a thousand kilometers. This holds true over many parts of the world's oceans and, where it is the case, vertical exchange processes between the air and the sea, as well as vertical mixing within the water column, are likely to affect local conditions much more rapidly and effectively than horizontal advection and horizontal mixing. It follows that it is permissible, for many purposes, to treat the upper ocean layers as being statistically homogeneous along the horizontal. This approximation is applied consistently in all models presented in this paper. It means that horizontal derivatives can be omitted in the mathematical treatment and only changes along the vertical are being considered.

It follows from the discussion in the Introduction (Chapter 1) that the prediction of the temperature is probably the most important function of upper ocean models. Temperature variations have a crucial effect on the climate, the local biological environment, and acoustic propagation. Next to temperature, we are concerned with current velocities in the upper ocean for shipping purposes, fish migration, and also for the modelling of the oceanic general circulation. However, for most of these purposes one wants to know not only the local current velocities but also their horizontal variations. The one-dimensional models are therefore generally less useful for the processing of velocity information than they are for temperature.

The temperature and velocity fields interact with each other and with the oceanic density field, which in turn is a function not only of temperature but also of salinity. In our models we have to deal therefore with the evolution of each of these properties. In the present context, this evolution can be described by a set of one-dimensional conservation equations. In particular the one-dimensional momentum equation can be reduced to the form:

$$\frac{\partial \bar{v}}{\partial t} + f \bar{k} \times \bar{v} + \frac{\partial}{\partial z} \overline{w'v'} = 0, \tag{10.1}$$

where \bar{v} is the averaged horizontal current velocity, f the Coriolis parameter and \bar{k} a unit vector along the vertical z direction. Primes are being used here to denote turbulent deviations from the bulk velocities \bar{w} and \bar{v} . Their averaged product represents the vertical flux of horizontal momentum, known as the Reynolds stress. The averages can be derived from time series segments of a few hours in the oceanic cases; shorter for laboratory experiments.

Because of the assumed horizontal uniformity $\partial \bar{w} / \partial z = -\nabla_H \cdot \bar{v} \approx 0$.

The conservation of sensible heat or enthalpy leads to the equation:

$$\frac{\partial \bar{T}}{\partial t} + \frac{\partial}{\partial z} \overline{w'T'} = -\frac{1}{\rho c} \frac{\partial I}{\partial z} \quad (10.2)$$

(\bar{T} =bulk temperature, ρ =density, c =specific heat, I =penetrating component of solar radiation). The fluctuating part of the temperature is denoted by T' . The last term in Eq. (10.2) is associated with a source of heat due to the absorption of solar radiation within the water column. As indicated by Ivanoff (Chapter 4), about 55 per cent of the incoming solar radiation is absorbed in the uppermost meter; the remainder penetrates deeper and is absorbed more or less exponentially with an attenuation coefficient γ which varies between about 0.03 m^{-1} in clear Mediterranean water and 0.3 m^{-1} in dirty coastal water. A value of $\gamma = 0.04 \text{ m}^{-1}$, corresponding to a scale depth of about 25 meters or slightly less, appears to characterize much of the open tropical and sub-tropical oceans.

The equation for the salinity S is

$$\frac{\partial \bar{S}}{\partial t} + \frac{\partial}{\partial z} \overline{w'S'} = 0. \quad (10.3)$$

Finally we shall require an equation which specifies mass conservation. However, as density fluctuations appear in the following equations always multiplied by the gravitational acceleration g , it is convenient to introduce an expression for the buoyancy

$$b = -g \frac{(\rho - \rho_r)}{\rho_r} \approx g(\alpha(T - T_r) - \beta(S - S_r)).$$

The subscript r denotes constant reference values of the density, temperature and salinity; the coefficients α and β describe the logarithmic expansion of ρ as functions of T and S respectively. The last identity can be used to derive a buoyancy conservation equation from the thermal and salinity equations:

$$\frac{\partial \bar{b}}{\partial t} + \frac{\partial}{\partial z} \overline{w'b'} = -\frac{g\alpha}{\rho c} \frac{\partial I}{\partial z}, \quad (10.4)$$

with b' denoting the fluctuating part of b . Below we shall assume $\rho \approx \rho_r$, except where the difference $\rho - \rho_r$ is needed for the specification of the buoyancy (Boussinesq approximation).

To solve the set of equations (10.1)-(10.4), one has to find explicit expressions for the turbulent fluxes. This has been attempted in a variety of ways which are listed below.

- a) **Deterministic solutions:** Basically this approach avoids the problem by a direct determination of the fluctuating velocities from the primitive equations. This requires specifications of the initial condition on a very fine space scale and computation of their evolution with a correspondingly high time resolution. This process has been used by Deardorff (1970) but it is too expensive and time

consuming to be utilized directly for routine oceanographic modelling and prediction.

- b) **Turbulence closure models:** As discussed briefly in the following section, these models involve the so-called Reynolds flux equations which express the evolution of the averaged products in Eqs. (10.1)-(10.4) as a function of higher order moments - that is, of averaged triple products - of the fluctuating quantities. These higher moments have to be parameterized in terms of empirical coefficients and computable quantities. This parameterization introduces some uncertainties and the equations are cumbersome.
- c) **Eddy coefficient and mixing length hypothesis:** This classical method, which is based on analogy with molecular transports, assumes that the turbulent fluxes can be expressed by the gradient of the transported quantity multiplied by an appropriate eddy diffusion coefficient:

$$-\overline{w'T'} = K_{MV} \frac{\partial \bar{T}}{\partial z}; \quad -\overline{w'S'} = K_V \frac{\partial \bar{S}}{\partial z};$$

and so forth. Developed more than fifty years ago, the method is still widely used (see, e.g., Holland, Chapter 2), though its physical basis is precarious. The main trouble is that the eddy transport coefficients are complicated functions of space and local stability conditions, which functions have to be determined empirically. This method breaks down when gradients vanish or when coupled fluxes of two conservative quantities transport one of them against its own gradient.

- d) **Mixed layer models:** Observations show that the top layer of the ocean is usually mixed rather thoroughly. The vertical distribution of temperature, salinity and horizontal velocity within this mixed layer is - if not uniform - at least very much smaller than the variations across the layer boundaries or variations within the thermocline below. Allowance for a uniform mixed layer permits vertical integration of Eqs. (10.1)-(10.4). This yields expressions for the turbulent transports in terms of the mean quantities and the external inputs. If $\partial I / \partial z = 0$, all transports within the mixed layer are linear functions of z . The turbulence energy equation (see next section) is used to obtain an expression for the evolution of the layer depth which is needed for closure.

The following section of this paper deals briefly with the turbulence closure schemes. The whole remainder is concerned with one-dimensional mixed layer models. At this stage of the art, these provide probably the most effective tool, particularly for the prediction of sea surface temperature and upper ocean heat storage over a relatively wide range of time scales.

10.2 Turbulence closure schemes

The full governing equations for the Reynolds stress tensor can be found for example, in a paper by Mellor (1973). Allowing for the here stipulated conditions of horizontal homogeneity and with neglect of the vertical component of the Coriolis force which cannot have any significant effect on the turbulent motion, these equations can be reduced to two separate

equations: one for the mean specific turbulence kinetic energy $q^2 \equiv \overline{w'^2 + v'^2}$ and a second one for the vertical transport of specific horizontal momentum $\overline{w'v'}$.

In the present case the turbulence kinetic energy equation has the form (Kraus, 1972):

$$\frac{1}{2} \frac{\partial}{\partial t} q^2 = - \overline{w'v'} \frac{\partial \bar{v}}{\partial z} + \overline{w'b'} - \frac{1}{2} \frac{\partial}{\partial z} [\overline{w'(w'^2 + v'^2)} + \rho \overline{w'p'}] - \epsilon. \quad (10.5)$$

The first term on the right-hand side represents the work of the stress $\overline{w'v'}$ on the mean shearing flow. As the kinetic energy of a shear flow is always larger than the kinetic energy of a uniform flow with the same average momentum, any reduction of the mean shear by mixing must generate an equivalent amount of eddy kinetic energy. The next term represents the rate of working of the buoyancy force. It is positive if relatively dense fluid parcels move downward while the lighter ones move upward. The following term deals with the convergence of the turbulent vertical flux which carries the energy of the turbulent velocity and turbulent pressure fluctuations. Finally, the last term represents the rate of viscous dissipation of turbulence energy. Explicit expressions for this dissipation, as found in textbooks of hydrodynamics, show that it involves also horizontal derivatives of the velocity fluctuations. However, these occur all in the form of squares and products, the averages of which do not disappear.

The corresponding one-dimensional equation for the Reynolds stress is:

$$\frac{\partial}{\partial t} \overline{w'v'} = -\bar{w}^2 \frac{\partial \bar{v}}{\partial z} - \frac{\partial}{\partial z} \overline{w'^2 v'} - \left(\overline{v' \frac{\partial p'}{\partial z}} + \overline{w'v'_H p'} \right). \quad (10.6)$$

The physical interpretation of the individual terms in this equation is less clear than in Eq. (10.5). The first right-hand term could be viewed as an averaged interaction between the perturbation vertical velocity and transient changes in the bulk current which are themselves produced by the vertical displacements. The second term clearly deals with the convergence of a turbulent vertical flux of Reynolds stress. The last term involves again the pressure correlations. Following an argument first made by Rotta (1951) this term can be expressed as a function of the double and triple velocity moments. It can be shown in this way that the principal effect of this term is to redistribute the energy between its components by conversion of the anisotropic disturbances associated with the shear and the buoyancy, into a more nearly homogeneous isotropic state. This has been discussed in more detail also by Lumley and Khajeh-Nouri (1974) and by Garwood (1976).

An exact presentation of the turbulence energy and Reynolds stress equations would include also terms for a viscous transport of energy and of Reynolds stress, as well as a term involving the vertical component of the Coriolis force. These terms are exceedingly small and quite irrelevant in the present context, though they can be found in Mellor's (1973) paper. That paper also contains the equations for $\overline{b'^2}$ and $\overline{w'b'}$ which correspond to Eqs. (10.5) and (10.6).

The set of equations (10.1)-(10.6) together with those for $\overline{b'^2}$ and $\overline{w'b'}$ is still not closed, because third order moments, like $\overline{w'v'^2}$ and $\overline{v'w'^2}$, have

been introduced as new unknowns. It would be possible, in principle, to represent the evolution of these third order moments by another set of equations which contain fourth order moments and so forth. As an alternative to such a rather futile exercise, one can try to close the system by a number of simplifying assumptions which approximate the third order moments as a function of the bulk variables, the second order moments and a variety of empirical constants. The mathematical treatment can be reduced further by assuming that the generation of the second order moments is in balance with their dissipation, that is, by omission of the time differentials and triple correlations in Eqs. (10.5) and (10.6). Mellor and Yamada (1974) have presented this whole process as a hierarchy of turbulence closure models which involve increasingly sweeping simplification. They show that it leads, at the lowest level, to the classical representation by eddy coefficients which are expressed as functions of a mixing length l and of the root mean square turbulent velocity q :

$$-\overline{w'v'} = K_{MV} \frac{\partial \bar{v}}{\partial z} \equiv l q S_{KM} \frac{\partial \bar{v}}{\partial z}, \quad (10.7)$$

$$-\overline{w'b'} = g \alpha K_V \frac{\partial \bar{T}}{\partial z} \equiv g \alpha l q S_K \frac{\partial \bar{T}}{\partial z}. \quad (10.8)$$

The factors S_{KM} and S_K represent the influence of the static stability on the eddy coefficients. As illustrated in Fig. 10.1 they are decreasing functions of the Richardson number

$$Ri = \frac{\partial \bar{b} / \partial z}{(\partial \bar{v} / \partial z)^2} \equiv \left(\frac{N}{\partial \bar{v} / \partial z} \right)^2. \quad (10.9)$$

The figure shows how widely estimates by various authors differ from each other. Munk and Anderson (1948) in particular assumed $lq = \text{const}$. When the number $Ri > 0$, work has to be done by the shear stress to mix a stably stratified fluid. Mellor's approach indicates that S_{KM} and S_K become zero for $Ri = 0.23$; this means that there can be no turbulent vertical transports of momentum or heat if Ri exceeds this critical value. In conditions of instability, the factors become infinite in the Munk and Anderson model. In Mellor's model they seem to approach asymptotically some limiting large value as $-Ri$ becomes large.

The most obscure and uncertain part of the formulation (10.7) and (10.8) is the concept of the mixing length l . At present there is no sound physical basis for a stipulation of this length as a function of the depth z . Mellor and Yamada (loc. cit.) use the interpolation formula

$$l = \frac{\kappa z}{1 + \kappa z / l_\infty} \quad (10.10)$$

($\kappa = 0.4$; von Kármán's constant). In this formulation $l \rightarrow l_\infty$ as $z \rightarrow \pm \infty$, with

$$l_\infty = m_1 \left(\int_0^\infty qz dz / \int_0^\infty q dz \right),$$

where m_1 is another empirical constant. Other possible formulations of l_∞ are listed by Kraus (1972), including one in terms of the Coriolis force and the gradient wind velocity by Blackadar who originally suggested the

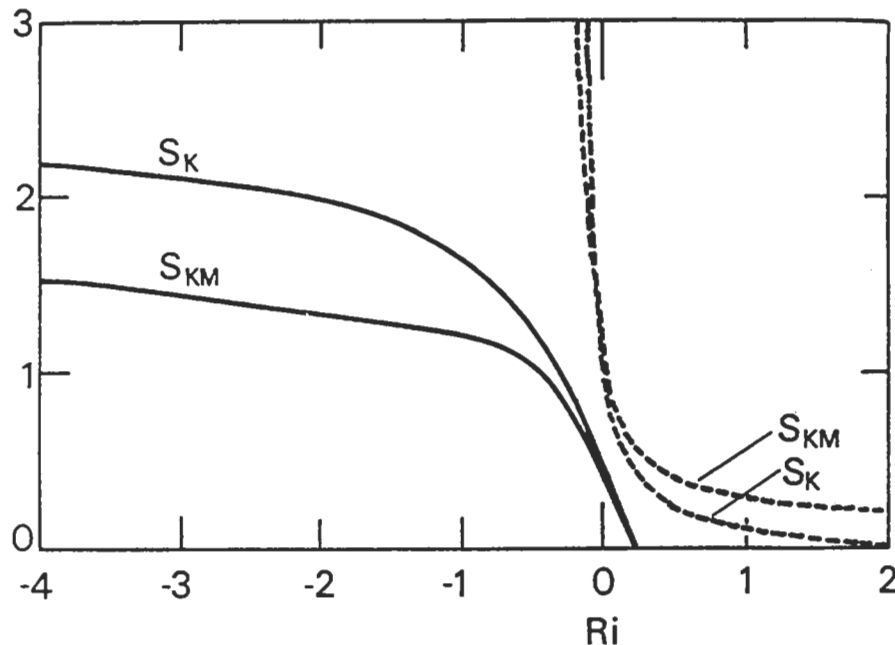


Fig. 10.1 - The stability factors S_{KM} and S_K (see Eqs. 10.7-10.9) as a function of the Richardson number Ri . The full lines are based on Mellor and Durbin (1975); the dashed lines represent the corresponding parameterization by Munk and Anderson (1948).

expression (10.10) and a somewhat different one in terms of the Coriolis force and the friction velocity by Lettau. All these formulations are rather arbitrary until they can be justified pragmatically.

If l is stipulated, the quantity q which also enters the expression for the K 's in Eqs. (10.7) and (10.8) can be obtained from the balanced turbulence energy equation ($d/dt=0$), if the triple and pressure correlations are neglected and the dissipation is set equal to $m_e q^3/l$. Equation (10.5) then assumes the form

$$\overline{w'v'} \cdot \frac{\partial \bar{v}}{\partial z} - \overline{w'b'} = \epsilon = m_e l^{-1} q^3. \quad (10.11)$$

In the last term, m_e is yet another empirically determined proportionality constant.

Equations (10.1), (10.4), (10.5), (10.7), (10.8), (10.11), together with the corresponding equation for \bar{b}'^2 , form a closed system which can be solved to yield the evolution of a velocity and temperature profile as a function of the atmospheric inputs and of the initial conditions. Pandolfo and Jacobs (1972) and Mellor and Durbin (1975) have carried out numerical experiments on this basis. These experiments do in fact develop reasonably realistic profiles

including mixed layers. However, apart from involving some rather arbitrary assumptions and at least three different empirical constants, the approach also requires a relatively complex computational scheme.

10.3 Mixed layer models

a. General considerations and assumptions

Vertically more or less uniform mixed layers can be found almost everywhere immediately below the ocean surface. We do not need a model to prove this fact. Its a priori acceptance greatly facilitates any modelling of the upper ocean. Mellor has pointed out that the resulting models are disconnected to some extent from the information which is available through general boundary layer theory, but this is compensated by the physical insight and simplicity which comes from their being tailored specifically for oceanic (and atmospheric) application.

An essential difference between the simplified equilibrium turbulence closure models and the layer models lies in the different physical importance which they assign to the transport of turbulence kinetic energy. To the extent that the equilibrium closure models omit all triple correlations, they arbitrarily set the flux of mechanical energy equal to zero. This leads to the reduced form (10.11) of the turbulence energy equation (10.5). On the other hand in the mixed layer models, turbulence energy which may have been supplied or generated indirectly by the wind near the surface is used to work against gravity at the bottom of the layer where dense water is entrained from below. The existence of a flux of turbulence energy is therefore essential to the mixed layer models. In the second order turbulence closure models, layer deepening can occur only if there is a "local" supply of energy because of a mean shearing motion at the bottom of the mixed layer.

The first mixed layer or bulk layer model developed by Keith Ball (1960) for the atmosphere above heated land did not in fact involve any mean horizontal motion. The approach was extended and modified for oceanic use by Kraus and Turner (1967). References to the following further development of mixed layer models, including consideration of horizontal shearing motions and observational evaluations, are listed in papers by Niiler (1975) and by Gill and Turner (1976).

It may be useful here to list explicitly the assumptions which have been made in most mixed layer models:

- i. The mean temperature, salinity and horizontal velocity are assumed to be quasi-uniform within the layer.
- ii. On the depth and time scales of the model, a quasi-discontinuous distribution can be envisaged for the same variables across the sea surface and across the lower mixed layer boundary.
- iii. The rate at which the mean square turbulent velocity (velocity variance) changes locally is assumed small compared to the turbulence generating and dissipating effects.
- iv. Temperature changes associated with frictional dissipation and with changes in salinity (chemical potential) are neglected.

The first two assumptions are characteristic for mixed layer models. The two others have also been made - explicitly or implicitly - in most turbulence closure or eddy coefficient schemes which have been used for oceanic modelling purposes (for an exception, see Weatherly, 1974).

Assumption (i), in particular allows us to integrate Eqs. (10.1)-(10.4) individually from the bottom of the mixed layer at a depth $z=-h$ to the surface at $z=0$. This permits representation of the bulk horizontal velocity \bar{v} , temperature T_0 and salinity S_0 of the layer as a function of exchanges with the air above and with the interior ocean below. The system is not closed, because the time-dependent depth h has been introduced as a new variable. In the absence of a mean vertical velocity ($\bar{w}=0$), any deepening of the layer must be equal to the rate w_e with which water is entrained from the interior below.

The physics of this entrainment has been discussed by Phillips (Chapter 7), including the fact that the entrainment flow can only be directed towards the more turbulent fluid region, that is, upwards in the present case. Entrainment is therefore associated with layer deepening. At times when the layer becomes shallower the entrainment must cease. Symbolically:

$$\begin{aligned} w_e &\equiv dh/dt && \text{for } dh/dt > 0; \\ w_e &\equiv 0 && \text{for } dh/dt \leq 0. \end{aligned} \quad (10.12)$$

To close the system, the entrainment velocity w_e is calculated from the vertical integral of the turbulence-energy equation (10.5) in its balanced form ($d/dt=0$). To evaluate the integrals of Eqs. (10.1)-(10.5) one has to know the flux boundary conditions at the surface ($z=0$) and at the bottom interface ($z=-h$).

b. Flux boundary conditions at the sea surface

The surface fluxes of sensible heat, salinity and the derived flux of buoyancy can be specified in most cases with reasonably good approximation by bulk aerodynamical formulae (Busch, Chapter 6) as functions of the existing atmospheric and mixed layer conditions:

$$\rho c \overline{w'T'} \Big|_{z=0} = R_0 - I_0 + H_0 + A_c Q_0 = R_0 - I_0 + \rho_a C_a u_a \{c_p [T_0 - T_a] + A_c [r_*(T_0) - r_a]\}; \quad (10.13)$$

$$\rho \overline{w'S'} \Big|_{z=0} = (P_0 - Q_0) S_0; \quad (10.14)$$

$$\overline{w'b'} \Big|_{z=0} = g \left\{ \alpha \overline{w'T'} \Big|_{z=0} - \beta \overline{w'S'} \Big|_{z=0} \right\} \equiv B_0. \quad (10.15)$$

The subscript 0 refers to conditions at the water surface, the subscript a refers to conditions in the air at some predetermined reference level $z=a$ (usually, $a \approx 10$ m). Most of the symbols have been explained in connection with Eqs. (10.1)-(10.4); the remaining ones have the following meanings:

R_0 = surface flux of solar and terrestrial radiant energy per unit area;

I_0 = surface flux of penetrating solar radiation ($\sim 45\%$ of total solar radiation);
 H_0 = surface flux of sensible heat;
 Q_0 = surface flux of water vapor (evaporation);
 A_c = latent heat of evaporation;
 C_a = surface drag coefficient;
 u_a = wind speed;
 P_0 = precipitation rate;
 r = specific humidity;
 r_* = saturation specific humidity.

The surface flux function B_0 specifies the rate at which buoyancy is removed from the water column (or available potential energy is supplied) by surface cooling and salinity changes:

$$B_0 \equiv \frac{g}{\rho} \left\{ \frac{\alpha}{c} (R_0 - I_0 + H_0) - \beta P_0 S_0 + \left(\frac{\alpha A_c}{c} + \beta S_0 \right) Q_0 \right\}. \quad (10.16)$$

All fluxes are considered positive when directed upwards from the water into the air. (This means that I_0 is always negative.) Because the heat capacity and density of water are very much larger than those of air, significant gradients can be sustained only in the atmosphere above the sea surface and not in the water. It is therefore permissible, for all intents and purposes, to equate the surface temperature and salinity with the bulk mixed layer values of these quantities.

In conditions of horizontal homogeneity, that is, on a fully developed sea, the magnitude of the downward flux of momentum from the surface is equal to the wind stress τ_0 . As such, it can be expressed in a variety of ways:

$$|\overline{w'v'}| = \frac{\tau_0}{\rho} \equiv u_*^2 = \frac{\rho_a}{\rho} C_a u_a^2, \quad (10.17)$$

where u_* is known as the friction velocity. When the wind blows with a speed $u_a = 8$ m s^{-1} at a height of 10 meters above the surface, $u_* \approx 1.0$ cm s^{-1} . The corresponding value of u_* in the air would be about 28 cm s^{-1} . The direction of the stress is equal to the wind direction close over the surface.

Finally we shall need an expression for the flux of the turbulent velocity and pressure fluctuations, given by the term in square brackets in Eq. (10.5). Near the sea surface, this flux must be equal to the rate of working by the wind. This means that it has to be equal to the stress multiplied by a wind velocity. The trouble is that one cannot measure this wind velocity without ambiguity at any particular height. The wind stress works on waves at heights which are different for waves of different length. Through tangential friction it also works directly on the surface (see Phillips, Chapter 12). In the circumstances it is inconvenient to be too specific at this stage. We shall describe the rate of working by the general relation:

$$\left[-\frac{1}{2} \overline{w'(w'^2 + v'^2)} + \rho^{-1} \overline{w'p'} \right]_{z=0} = m_1 u_* \quad (10.18)$$

leaving consideration of the proportionality factor m_1 for discussion below.

c. Flux boundary conditions at the bottom of the mixed layer

We shall neglect the effect of diffusion across the stable interface at the bottom of the mixed layer and assume that all mixing processes are associated with the entrainment of the lower fluid into the mixed layer. The boundary conditions for the flux of heat, salinity, and buoyancy assume then the forms:

$$\left. \begin{aligned} \overline{w'T'} \Big|_{z=-h} + w_e \Delta T &= 0 \\ \overline{w'S'} \Big|_{z=-h} + w_e \Delta S &= 0 \\ \overline{w'b'} \Big|_{z=-h} + w_e \Delta b &= 0 \end{aligned} \right\} \quad (10.19)$$

The symbols ΔT , ΔS and Δb represent the quasi-discontinuous changes of these three quantities across the base of the mixed layer.

In the absence of entrainment, all the turbulent fluxes become zero at $z=-h$. In physical terms, this means that there is just not enough turbulence energy available in this case to overcome the stable stratification at the base of the layer and to produce any mixing with the lower water. The mixed layer becomes then effectively decoupled from the ocean interior. In the model presented here, this decoupling is assumed to be absolute.

The momentum flux boundary condition is not quite as simple. As discussed by Pollard and Millard (1970), internal waves can radiate momentum downwards through stable layers even in conditions of horizontal homogeneity. Integrated over some time, the resulting bottom drag on the mixed layer can be of the same order as the acceleration produced by the wind. It may contribute to the relatively fast attenuation of the inertial oscillation which can be produced in the mixed layer by sudden wind changes. Following Crepon*, we shall parameterize this radiation stress by the square of \bar{v} , multiplied by a generalized drag coefficient C , which should be a function of the particular density stratification in the fluid below the mixed layer. This parameterization is rather crude; fortunately it will be seen below that it has little effect on the features with which our model is primarily concerned. The momentum flux boundary conditions, as derived from this argument, becomes

$$\overline{w'v'} \Big|_{z=-h} + w_e \bar{v} = C \bar{v} |\bar{v}|. \quad (10.20)$$

Finally, the boundary condition for the flux of mechanical energy can be established similarly in the form

$$\left[\frac{1}{2} \overline{w'(w'^2 + v'^2)} + \rho^{-1} \overline{w'p'} \right]_{z=-h} + \frac{1}{2} w_e q^2 = 0. \quad (10.21)$$

The second term represents here the rate at which turbulence energy has to be supplied by the downward flux to make the entrained (initially quiescent) water as agitated as the mixed layer water.

d. The integral relations

To obtain explicit expressions for the mixed layer momentum, temperature, salinity, and buoyancy, one integrates Eqs. (10.1)-(10.4) along the vertical. The integration is easy because the bulk variables are independent of z within the mixed layer. To deal with the effect of penetrating solar radiation we set

$$I = I_0 \exp(\gamma z),$$

as discussed in Section 10.1. The mixed layer temperature must then satisfy the equation

$$\frac{dT_0}{dt} = -\frac{w_e \Delta T}{h} - \frac{1}{\rho c h} (R_0 + H + A_0 Q_0 - I_0 e^{-\gamma h}). \quad (10.22)$$

The first term on the right hand side represents the temperature decrease in the layer which is caused by the entrainment of water with a temperature that is ΔT lower than T_0 . The term in brackets represents the flux of heat through the sea surface minus the penetrating solar radiation which passes, through the layer into the deeper water below the level $z=-h$. In the following computations it will be assumed that $\gamma h \gg 1$, and that $\exp(-\gamma h)$ is therefore negligibly small.

The equation for the salinity has the form

$$\frac{dS_0}{dt} = -\frac{w_e \Delta S}{h} + \frac{S_0}{\rho h} (Q_0 - P_0). \quad (10.22')$$

The corresponding integral equations for the buoyancy b and the mean momentum $\rho \bar{v}$ can be written down without difficulty.

To close the system, one needs an expression for w_e . This can be obtained from an integral of the turbulence energy equation (10.5) in its balanced form ($d/dt=0$). An integral of the vertical buoyancy flux $\overline{w'b'}$ which occurs in Eq. (10.5) can be obtained by integrating Eq. (10.4) from a depth Z to the surface and again from the depth $-h$ to the surface. The time derivative db_0/dt can then be eliminated between these two integrals. After rearrangement one gets:

$$\overline{w'b'} = B_0 + \frac{Z}{h} (B_0 + w_e \Delta b + \frac{g\alpha}{\rho c} I_0) + \frac{g\alpha}{\rho c} I_0 (1 - e^{-\gamma Z}). \quad (10.23)$$

For simplicity, we set $J_0 = \frac{g\alpha}{\rho c} I_0$ and integrate Eq. (10.23) from the bottom of the layer $z=-h$ to the surface $z=0$, obtaining

$$\int_{-h}^0 \overline{w'b'} dz = \frac{1}{2} h B_0 - \frac{1}{2} w_e \Delta b h + J_0 \left(\frac{h}{2} - \frac{1}{\gamma} \right). \quad (10.24)$$

The last equation represents the rate of potential energy change associated with the lifting or lowering of the center of gravity of the water column by convection. The first term on the right hand side is the contribution of the surface flux to the potential energy change. This contribution is positive when the surface is cooled ($B_0 > 0$). The second term represents the reduction of potential energy caused by the lifting of the dense entrained water. The product

$$Abh = c_1^2, \tag{10.25}$$

where c_1 is the velocity of the long internal waves at the bottom interface $z=-h$. Finally, the last term represents the change which is due to the absorption of solar radiation in depth and to the redistribution of the resulting heat increase by convection. This redistribution increases the potential energy if the penetration scale length γ^{-1} exceeds the half depth of the mixed layer, and vice versa.

The derivation of an explicit expression for the flux and the generation of turbulence kinetic energy is not as straight forward, because the generating term $\overline{w'v'} \cdot \frac{\partial \overline{v}}{\partial z}$ is obviously zero in the interior of the layer, if the layer moves indeed uniformly like a slab. On the other hand in the transition zone at the bottom of the layer which is illustrated in Fig. 10.2, $\frac{\partial \overline{v}}{\partial z} \rightarrow \infty$ as $(h'-h) \rightarrow 0$. From Eq. (10.20) we deduce that

$$\lim_{(h'-h) \rightarrow 0} \int_{-h'}^{-h} -\overline{w'v'} \cdot \frac{\partial \overline{v}}{\partial z} dz = \frac{1}{2} w_e \overline{v}^2 + \frac{1}{3} c |\overline{v}|^3. \tag{10.26}$$

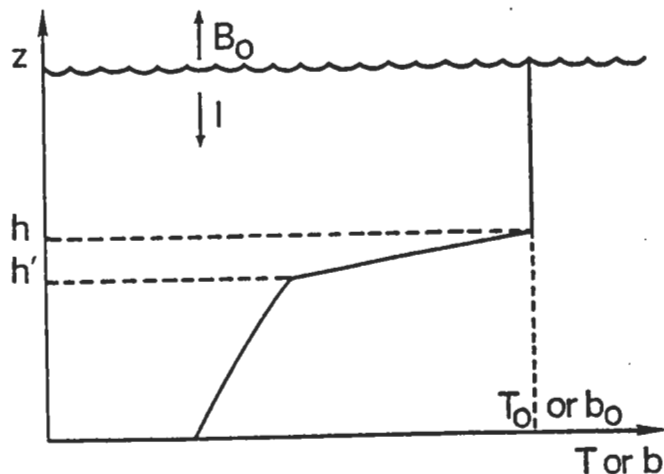


Fig. 10.2 - Schematic of mixed layer model.

Turbulence energy is also likely to be produced by the mixing of shear flows near the surface. However, in reality this must always involve running waves, and if a sea is present it cannot be modelled analytically. Fortunately, one can assume that the rate of generating of mean shearing motion near the surface will be equal to the rate of its destruction by mixing. This makes the turbulence production term proportional to the rate of working by the wind. Its effect can be accounted for by an adjustment of the proportionality constant in the relation (10.18).

On the basis of the preceding argument and with the assumption of a discontinuous interface it is now possible to write the integrated turbulence energy equation in the form

$$\frac{1}{2} w_e (q^2 + c_1^2 - \overline{v}^2) = m_1 u_*^3 + \frac{1}{2} h B_0 + \left(\frac{h}{2} - \frac{1}{\gamma}\right) J_0 - C |\overline{v}|^3 - \int_{-h}^0 \epsilon dz. \tag{10.27}$$

A B C D E F G H

Equation (10.27) looks cumbersome; fortunately it can be very much simplified in almost any particular case, because the individual terms tend to have unequal magnitudes. Before this is shown below, it may be useful to recapitulate once more the meaning of these terms:

- A: rate of energy needed to agitate the entrained water (Eq. 10.21);
- B: work per unit time needed to lift the dense entrained water and to mix it through the layer (Eqs. 10.24 and 10.25);
- C: rate at which energy of the mean velocity field is reduced by mixing across the layer base (Eq. 10.26);
- D: rate of working by the wind (Eq. 10.18);
- E: rate of potential energy change produced by fluxes across the sea surface;
- F: rate of potential energy change produced by penetrating solar radiation (Eq. 10.24);
- G: rate of working of radiation stress associated with internal waves (Eq. 10.20);
- H: dissipation.

e. Parameterization of the dissipation

If the most arbitrary link in the second order turbulence closure models has been the specification of a mixing length, the same might be said about the dissipation in the integral or mixed layer models. From dimensional arguments dissipation can be expected to be proportional to the third power of the mean turbulence velocity. The turbulent agitation is most intense close to the regions where turbulence energy is generated; for example, when the turbulence is due to wind stirring, its intensity tends to decrease with distance from the surface. The opposite holds when turbulence is caused by some interior shear. On the basis of such observations, it will be assumed here that the dissipation integral is composed of terms which are individually proportional to the active turbulence generating processes, that is, to the

terms C and D and also to E during periods of active cooling when B_0 is positive. Formally:

$$\int_{-h}^0 \epsilon dz = (m_1 - m) u_*^3 + (1-s) \frac{1}{2} w_e \bar{y}^2 + (1-n) \frac{1}{2} h \frac{B_0 + |B_0|}{2}. \quad (10.28)$$

The proportionality factors have been written in the particular forms $(m_1 - m)$, $(1-s)$, and $(1-n)$ for the sake of convenience, because this simplifies the expressions to follow. They are not necessarily constant and it will be seen below that they may assume different numerical values which depend on the layer depth and the magnitude of the forcing. Actual values have to be established empirically from laboratory experiments and field observations. The last term in Eq. (10.28) should differ from zero only when turbulence is generated by surface cooling ($B_0 > 0$); this is the reason why it has been

written in the peculiar form shown. It may be appropriate to list here some other proposed parameterization schemes. One, suggested by Niiler (1975) and in a slightly different form by Kim* (1975) has the form

$$\int_{-h}^0 \epsilon dz = C_e u_*^3 \exp\left(-\frac{h}{h_0}\right) + \epsilon_0 h,$$

where C_e is another proportionality factor, ϵ_0 is a "background" dissipation rate, and h_0 is a decay scale for dissipation as a function of depth based on field experiments by Grant, et al. (1969). This formulation relates the dissipation only to the working of the wind and not to other turbulence generating processes. It also will be seen below that even in the case of a purely mechanical energy input, it is not supported by experimental results.

Another scheme by Garwood* (1976) introduces a dissipation rate which is proportional to q^3/h . This is in keeping with other turbulence studies. He stipulates an entrainment rate of the form

$$\frac{w_e}{w_*} = \frac{q^2}{c_i^2},$$

where w_* is the geometric mean of the vertical component of turbulent velocity close to the layer bottom. The quantities w_* and q have to be determined separately. Readers are referred to the original paper for details of the procedure.

At this stage of the art, the formulation (10.28) is preferred. Though rather crude, it is relatively simple and it incorporates just about all that can be said with any confidence about the underlying physical processes. Introduction of Eq. (10.28) into Eq. (10.27) yields

$$\frac{1}{2} w_e (q^2 + c_i^2 - s \bar{y}^2) = \underbrace{m u_*^3}_A + \underbrace{\frac{h}{2} [(1+n)B_0 - (1-n)|B_0|]}_B + \underbrace{\left(\frac{h}{2} - \frac{1}{Y}\right) J_0}_C + \underbrace{\frac{1}{2} C |\bar{y}|^3}_D. \quad (10.29)$$

This expression can be simplified further, because the first and the last terms are relatively small in most circumstances. In particular, the mean square turbulent velocity q^2 in the upper ocean is typically of order $10^0 \text{ cm}^2 \text{ s}^{-2}$. It never exceeds $10 \text{ cm}^2 \text{ s}^{-2}$. On the other hand c_i^2 is of order $10^3 \text{ cm}^2 \text{ s}^{-2}$ even if the layer is only 10 meters deep. It becomes larger as the layer gets deeper. A layer depth of at least a few meters is assured by the slightest amount of surface cooling or wind stirring (see Sections 10.4a and 10.5a below). It follows that almost invariably $c_i^2 \gg q^2$, allowing us to neglect term (A) in all the considerations below.

In dealing with term (G) we are on weaker ground. This term is related to the rate of working of the shear stress at the layer bottom, as indicated by Eq. (10.26). Anticipating again the discussion below, one can say that most of the time in the oceans, the rate of energy input by the wind through the sea surface is likely to be very much larger than the rate of energy production by the internal shear stress. However, this may not hold true during certain stages of the development when $|\bar{y}|$ becomes relatively large.

We shall assume that when this happens term (G) remains relatively small compared to term (C); that is $w_e \gg C |\bar{y}|$. In physical terms this implies that the energy which is generated by the working of the shear stress is either dissipated locally or used to entrain dense water from below with relatively little being radiated away. Following these considerations we shall assume that the radiational drain of energy is small and that its effect can be incorporated in the empirical factor S.

With these assumptions one can write the last equation in the form

$$w_e (c_i^2 - s \bar{y}^2) = \underbrace{2m u_*^3}_B + \underbrace{\frac{h}{2} [(1+n)B_0 - (1-n)|B_0|]}_C + \underbrace{\left(h - \frac{2}{Y}\right) J_0}_D. \quad (10.30)$$

The Roman letters have the same meaning as in Eq. (10.27), although the relevant terms include now the effects of dissipation. Term (E) equals hB_0 when $B_0 < 0$; it is equal to nhB_0 when $B_0 > 0$. It is in the form (10.30) that the turbulence energy equation will be applied below.

10.4 Mixed layer modelling of special cases and particular circumstances

The Eqs. (10.12), (10.16), (10.22), (10.22') and (10.30) form a closed system for B_0 , T_0 , S_0 , h and w_e . Another equation for the layer momentum \bar{y} can be added. To simplify evaluation we distinguish between periods when the heating increases, and when it decreases or when cooling occurs. During the

former periods, the layer tends to become shallower ($dh/dt < 0$); there is no entrainment in this case ($w_e = 0$) because there is not enough energy available to work against the increasing stability. The temperature and salinity will vary continuously across the layer base, though there will be a discontinuity in their gradient. Energetically, the layer is decoupled from the lower water during these periods.

During periods of decreasing heating or cooling, conditions depend crucially on the depth h . The terms (B) and (E) both tend to increase with increasing layer depth. The other terms are either independent of h or they decrease as the layer gets deeper. One can therefore expect a balance between (B) and (E) in late fall, for example, when the layer is relatively deep. Another controlling factor is the relative magnitude of the wind stirring and the thermal forcing, as expressed by the ratio

$$\frac{2u_*^3}{B_0 h} \equiv \frac{L^*}{h}, \quad (10.31)$$

where L^* can be interpreted as a generalized Monin-Obukhov length. When L^*/h is large, the turbulence is dominated by wind stirring; thermal convection becomes the dominant factor when the ratio is small and positive. ~~negative~~

We shall now consider some of the various possibilities:

a. Increasing stability - no wind

On a calm morning or during windless spring days when the sea is being heated by radiation ($R_0 < 0$), the layer depth tends to decrease ($dh/dt < 0$).

There can be no entrainment in this case ($w_e = 0$), and all the terms in Eq. (10.30) except (E) and (F) are therefore zero. It follows that the depth h and the flux function B_0 must adjust themselves in a way which make the sum of these two terms also equal to zero. In the absence of wind, the evaporation and the turbulent flux of sensible heat from the sea surface are likely to be small as well. The value of B_0 in Eq. (10.16) is then determined approximately by radiation alone.

Two cases have to be distinguished depending on the sign of the surface infrared radiation balance ($R_0 - I_0$), which is also the sign of B_0 . If ($R_0 - I_0$), and therefore B_0 , is negative, the surface is being heated by infrared radiation. Without any heat sink within the water, the enthalpy flux and the buoyancy flux must be directed downward ($w^*b^* < 0$). The balanced turbulence energy equation (10.5) can then not be satisfied, because there is no energy source available to transport buoyancy downward. In other words there can be no mixed layer present: $h=0$ if $B_0 < 0$ and $u_* = 0$.

If $R_0 - I_0$ and B_0 are positive, one gets from the sum of the terms (E) and (F) after rearrangement

$$h = \frac{2}{\gamma} \frac{J_0}{nB_0 + J_0} = \frac{2}{\gamma} \frac{I_0}{n(R_0 - I_0) + I_0}. \quad (10.32)$$

If there is no dissipation ($n=1$), one sets

$$h = \frac{2}{\gamma} \frac{I_0}{R_0}.$$

On the other hand, if all the convectively generated energy is dissipated locally ($n=0$), the layer depth tends to become equal to double the penetration scale length

$$h = \frac{2}{\gamma}.$$

To compute the temperature rise, one eliminates h between Eqs. (10.22) and (10.32). With the radiation flux through the base of the layer considered very much smaller than the radiation balance at the surface, one gets, with $w_e = 0$:

$$\frac{dT_0}{dt} = - \frac{R_0 \gamma}{\rho c} \frac{n(R_0 - I_0) + I_0}{2I_0}. \quad (10.33)$$

The case represented by the Eqs. (10.32) and (10.33) was first modelled by Kraus and Rooth (1961) who also list empirical expressions for R_0 as a partial function of T_0 . Although Eq. (10.32) is a balance equation, h is not necessarily constant, but changes with R_0 and therefore with T_0 . The temperature change dT_0/dt is always positive during the adjustment process (active heating).

b. Decreasing stability - no wind

During night $I_0 = 0$; the convective energy generation minus dissipation which is represented by term (E) in Eq. (10.30) is balanced by the entrainment of dense water as represented by term (B). It follows that:

$$w_e = \frac{nhB_0}{c^2} = \frac{nB_0}{\Delta b}. \quad (10.30')$$

With active entrainment, $w_e = dh/dt > 0$ (see Eq. 10.12). The form of B_0 is specified by Eq. (10.16). In the circumstances envisaged here, B_0 is dominated by infrared cooling ($B_0 \approx R_0$; $\Delta b = \Delta T$). The last equation is therefore equivalent to:

$$\frac{dh}{dt} = \frac{n}{\rho c} \frac{R_0}{h}. \quad (10.34)$$

Introduction of this expression into Eq. (10.22) yields:

$$\frac{dT_0}{dt} = \frac{1+n}{2\rho c} \frac{R_0}{h}. \quad (10.35)$$

It is easy to add the appropriate terms for the sensible heat loss and evaporation to R_0 on the right hand side of the Eqs. (10.34) and (10.35) if

these processes are significant. However, it should be noted, that even in the present simple case the pair of Eqs. (10.34) and (10.35) generally can only be integrated numerically. In particular, R_0 is a nonlinear function of T_0 and also depends on the atmospheric conditions; ΔT depends not only on T_0 but implicitly also on the layer depth h and on the temperature gradient below.

The argument leading to the expressions (10.34) and (10.35) was first developed by Ball (1960) in a model of atmospheric temperature changes over heated land. Instead of cooling at the upper surface of the fluid, the forcing is brought about in his case by the convective heating from the isolated land surface. Ball assumed that the resulting free convection is carried by large eddies which are not affected at all by dissipation. With our present terminology this would imply $n=1$.

The opposite extreme would be to assume that all the convectively generated energy is dissipated within the layer. This is tantamount to setting $n=0$. There is then no energy available for entrainment and the rate of temperature change dT_0/dt is only half as fast as for $n=1$. However, as shown, for example, by Lilly (1968), with somewhat different nomenclature for the atmospheric case, the final mixed layer temperature which is established may not differ very much in the two cases.

c. Increasing stability - with wind

We shall assume that the wind stirring is insufficient to produce entrainment ($w_e=0$) in the presence of strong radiational heating. The layer depth must then become shallower until h has decreased to a value which keeps the right-hand side of Eq. (10.30) equal to zero.

For the case of surface heating ($B_0 < 0$), one gets from Eq. (10.30)

$$h = \frac{-2\mu_*^3 + 2J_0/\gamma}{B_0 + J_0} \quad (10.36)$$

During night or in heavy overcast conditions $J_0=0$. Equation (10.30) then reduces - with consideration of the expression (10.31) - to

$$h = -\frac{2\mu_*^3}{B_0} = -mL^* \quad (10.37)$$

This means that the layer should become stabilized when it has a depth which corresponds to the Monin-Obukhov length. Kitaigorodskii (1960) suggested that this should be the fundamental scale depth of the ocean mixed layer - one in which just sufficient mechanical energy is available from the wind to mix the heated surface water uniformly down to a depth $h=L^*$.

The layer temperature T_0 and surface salinity S_0 can be evaluated by introducing Eq. (10.36) or (10.37) into (10.22) and (10.22') with $w_e=0$ and with an explicit expression for B_0 as specified in Eq. (10.16).

When the surface is cooled ($B_0 > 0$) in the presence of wind, the layer tends to deepen ($w_e \neq 0$). This case will be discussed in Section 10.4e below.

d. The effect of inertial currents in the mixed layer

Any wind change generates inertial currents in the upper ocean. Their presence tends to produce a sharp velocity gradient at the layer bottom interface. When this happens, the term (C) in Eq. (10.30) must be considered.

The contribution of shear stresses at the bottom of the layer, to the work of layer deepening was investigated first by Pollard, Rhines and Thompson (1973). They argued that these stresses feed energy into finite-amplitude perturbations, which break up the interface when the ratio of the hydrostatic stability to the shear instability - that is the local Richardson number - drops below some critical value. The break-up speeds up the entrainment process, causing an adjustment of the layer depth which prevents any further increase of the velocity shear beyond its critical value. While the deepening proceeds, the work of the shear stress is used mainly to lift the dense water from below. Pollard, et al. equated the critical local Richardson number with the bulk Richardson number

$$Ri_* = \frac{\Delta b h}{\bar{v}^2} = \left(\frac{c_1}{\bar{v}}\right)^2 \quad (10.38)$$

Using this expression to eliminate c_1 from Eq. (10.30) one gets

$$w_e (Ri_* - s) \bar{v}^2 = 2\mu_*^3 + nhB_0 \quad (10.30'')$$

For a given rate of surface forcing, a small value of the difference $Ri_* - s$ must be associated with large values of w_e and therefore with rapid layer deepening.

For simplicity's sake, the solar heating term (F) has been omitted in Eq. (10.30''). It represents a process which is unlikely to be important during storm driven layer deepening. Retention of this term, when that is desirable, does not involve any additional analytical difficulties, but it does make the resulting expressions longer and more cumbersome.

To obtain an explicit expression for \bar{v}^2 one integrates Eq. (10.1) over the layer depth with the boundary conditions (10.17), (10.20) and over time with the initial condition $\bar{v}=0$ for $t=0$. The result in symbolical form is:

$$|\bar{v}| = \frac{u_*^2}{\pi h} (e^{-ift} - 1) \quad (10.39)$$

The radiation term $C\bar{v}^2$ which occurs in the boundary condition (10.20) has been neglected in this derivation. The squared modulus of Eq. (10.39) is

$$\bar{v}^2 = \frac{2u_*^4}{h^2\pi^2} (1 - \cos ft) = \frac{\Delta b h}{Ri_*} \quad (10.40)$$

The last equality follows directly from (10.38). Rearrangement yields

$$h = [Ri_* \frac{2u_*^4}{\Delta b f^2} (1 - \cos ft)]^{1/3}, \quad (10.41)$$

In their original paper, Pollard, et al. assumed arbitrarily that

$$Ri_* = 1, \quad (10.38')$$

which is tantamount to setting $\bar{v}^2 = c_f^2$. This restriction was abandoned in later papers.

To evaluate Eq. (10.41) explicitly one has to use a second independent relation which connects the two dependent variables h and Δb . Regardless of this complication, the expression (10.41) would suggest that the layer reaches a maximum limiting depth h_f when $t = \pi/f$, that is, one half of a pendulum day after the onset of the inertial oscillation. Inertial motions can only play an important role in the deepening process if the initial depth $h(t=0) < h_f$.

e. The erosion of deep mixed layers

As the layer deepens further, c_f^2 tends to increase with h while \bar{v}^2 decreases in inverse proportion to h^2 . The contribution of the velocity shear to the layer deepening tends therefore to become small as h increases beyond h_f . Omission of \bar{v}^2 at this stage and division by $c_f^2 = h\Delta b$, changes Eq. (10.30'') into

$$\frac{dh}{dt} = w_e = \frac{2mu_*^3}{h\Delta b} + \frac{nB_0}{\Delta b}. \quad (10.30''')$$

This was the equation used by Kraus and Turner (1967) in their model of the deepening layer.

Consider first the case when wind stirring predominates. In terms of Eq. (10.31) one has then $h \ll L^*$ which allows us to neglect the last term in Eq. (10.30'''). We divide by u_* and obtain then

$$\frac{w_e}{u_*} = 2m \frac{u_*^2}{h\Delta b} = 2m Ri_*^{-1} \quad (10.42)$$

This equation is equivalent to Eq. (7.6) in Phillips' treatment of entrainment, with Ri the bulk Richardson number as defined there. From the discussion there - to be recapitulated below - it follows further that m is not constant, but becomes smaller at high Richardson numbers. With m known empirically from the laboratory experiments, one can again compute the changing layer depth and temperature by integration of Eqs. (10.22) and (10.42).

Continued deepening must ultimately cause the first term on the right-hand side of Eq. (10.30''') to become small compared to the last one. In

other words, as h continues to grow it must become larger than L^* . Wind stirring then becomes irrelevant for further deepening, and the entrainment equation assumes again the form (10.30') which as established in Section 10.4b for a shallow layer with no wind above:

$$\lim_{h \rightarrow \infty} (w_e) = n \frac{B_0}{\Delta b}.$$

If one sets $n=1$, the last expression approaches once more Ball's (1960) original formulation. Gill and Turner (1976) argue convincingly that this original formulation cannot be representative at all times. They show that neglect of dissipation during layer deepening - in our terms $n=1$ - would be associated with an ever increasing potential energy. They propose, therefore, that at this stage there is a balance between convective energy generation and dissipation. Such a balance would imply that $n=0$, and as a discontinuity could not be maintained in these circumstances, one also has $\Delta b=0$. Below it will be argued that $n=1$ and $n=0$ are extremes which are approached at different stages of the development with $n \rightarrow 0$ as $h \rightarrow \infty$.

10.5 The proportionality factors - comparison with laboratory and field experiments

The preceding analysis involved three proportionality factors m , n and S , which have to be established empirically. Most of the experimental work so far has concentrated on the determination of the factor m . Laboratory experiments by Kato and Phillips (1969) suggested a value $m=1.25$. Later experiments by Kantha* (1975) are described in Phillips' Chapter 7. They do show that m is not constant. To compare the results with the present analysis, one must consider that B_0 was zero in Kantha's experiments. Equation (10.42) is relevant in these circumstances. When this equation is compared with the plot of Fig. 7.2, one finds that a line with a constant slope of $2m=2.5$ coincides with the axis of the shaded area which represents Kato's and Phillips' original experiments. The later results indicate that m is rather larger than originally estimated and that it is a decreasing function of the ratio $c_f^2/u_*^2 = h\Delta b/u_*^2$.

$$m \equiv m \left(\frac{h\Delta b}{u_*^2} \right). \quad (10.43)$$

When this ratio is of order one hundred, m is about 3.3. The experimentally determined values of m become smaller as the ratio $h\Delta b/u_*^2$ increases.

For the interpretation of field observations, it is more convenient to express the working of the wind not in terms of u_* but in terms of the actually measureable wind velocity u_a at the level $z=a$ above the surface. Denman and Miyake (1973), for example, use the expression

$$mu_*^3 = m_a (\rho_a C_a / \rho)^{1/2} u_a^3.$$

They calculated that a value of $m_a=0.0015$ corresponded to a value of $m=1.25$. A slightly smaller value of $m_a=0.0012$ gave a reasonably good fit for their analysis of records from ocean weather station Papa ($50^\circ N$, $145^\circ W$). The same

value also fitted the results of Denman's (1973) idealized wind mixing studies. On the other hand, Turner (1969) found that a considerably larger value of $m_a \approx 0.01$, corresponding to $m \approx 8$ would be necessary to account for rapid storm-induced deepening of the mixed layer which had been observed by Stommel, et al. (1969) in the Sargasso Sea. In a similar way a rapid increase in the mixed layer depth which had been reported by Halpern (1974b) to have occurred in August off the west coast of N. America, could be interpreted as due directly to wind mixing only if one were to stipulate a value of the proportionality factor m which is much in excess of the laboratory experiments.

The contradiction between the laboratory experiments and some of the oceanic observations - particularly those characterized by rapid deepening - may be caused by the interface destabilization which is produced by the working of the shear stress at the bottom of the mixed layer. This can be associated in turn with transient shears produced by internal waves as suggested in Kantha's note below, or with inertial currents in the mixed layer. If allowance is made for these additional processes, which can be important if $h < h_f$ initially, one is faced with the need to evaluate the factor s . Unfortunately we have hardly any experimental data for this purpose.

It is encouraging that Pollard and Millard (1970), Halpern (1974) and Begis and Crepon* in the Mediterranean all found that during the first few inertial oscillations after a storm passage, the mixed layer does in fact tend to move like a slab with little vertical velocity shear. This means that all the shearing motion is concentrated at the bottom of the layer and Eq. (10.40) is applicable. The question is how much of the shear-produced energy release remains available for entrainment?

Pollard and Wyatt* (1976) based a tentative answer on the assumption

$$m \approx s \approx Ri = \Delta b h / \bar{v}_*^2.$$

In the absence of surface cooling $B_0 \approx 0$, Eq. (10.39) assumes then the form

$$\frac{w_e}{u_*} = \frac{2s}{1-s} \left(\frac{u_*}{\bar{v}} \right)^2. \quad (10.44)$$

Equation (10.44) allows determination of s as a function of time during periods when the layer deepening is in fact dominated by the production of turbulence kinetic energy from shearing motion at the lower layer boundary.

To carry out their assessment, Pollard and Wyatt used measurements of dh/dt , u_* and \bar{v} which had been obtained during the 1972 JASIN experiment in the North Atlantic. The results suggest $s < 1$. This is in agreement also with the results of a study by Shonting and Goodman* in the Mediterranean. As of present, the best series of observations were obtained probably by Price*, Mooers, and Van Leer (1976) in the Gulf of Mexico. From simultaneous measurements of the temperature structure and of the inertial current velocity, Price found that $s \approx 0.7$ gave the best fit. As mentioned above, the factor s is affected not only by the dissipation but also by the drain of energy caused by internal wave radiation downward from the mixed layer base. This being the case, one would expect s to be a function not only of \bar{v}^2 but also of the stability in the water immediately below the depth $z = -h$.

As regards the factor n , several authors - starting with Ball - assumed

$n=1$. This assumption was based on the rationale that the convectively produced eddies are too large in size to be much affected by dissipation. On the other hand, Gill and Turner found that $n=0$ gave a good fit to the data presented here as Fig. 10.4 (below). Deardorff, Willis, and Lilly (1969) carried out laboratory tank experiments which yielded $n=0.015$. Farmer (1975), observing the deepening of a mixed layer under the ice of a frozen lake, found values of $0.003 \leq n \leq 0.113$ with a mean of $n=0.036$ for his series of twelve observations.

Tentatively, we suggest that the factor n exhibits a behavior which is similar to that of m , and that it is a decreasing function of the ratio between the relevant kinetic energy consuming and energy producing terms. It therefore should go towards zero as h becomes large. This suggestion is speculative. If it is thought acceptable, one has still to distinguish between forced and free convection.

The case of forced convection is represented by Eq. (10.30'''). In this case w_e can be scaled by u_* , and n is then presumably a function of the form

$$n \approx n \left(\frac{B_0}{u_* \Delta b} \right). \quad (10.45)$$

In the case of free convection ($u_* = 0$) which applies to the quoted observational studies, one has to scale w_e by a convective velocity which is proportional to the cube root of (hB_0) . If n is to be a function of the work terms, it must have the form

$$n \approx n (B_0^{2/3} h^{-1} \Delta b^{-1}). \quad (10.46)$$

From the preceding discussion one would expect n to be a decreasing function of its argument, that is $n \rightarrow 0$ as $h \rightarrow \infty$, in analogy with the behavior of the factor m .

In view of the uncertainties about the factors m , n and s , it is rather fortunate that the one-dimensional mixed layer models are not very sensitive to the actual value of these quantities. Particularly in those cases where a new equilibrium is being developed by the model, as a result of changes in the forcing function, it will be the rate of approach to this equilibrium rather than its final character which can be affected by the actual numerical value of the proportionality factors.

It is obvious that there is scope for further research on the functional form of the factors m , n and s ; or for the matter on the whole problem of representing dissipation as a parametric function of the bulk variables. An elucidation of these problems is most likely to come from further laboratory experiments and from oceanic observations carried out over a wide range of different circumstances. Work on the downward mixing of fresh water lenses produced by tropical showers as illustrated by Fig. 10.3 and the studies of mixed layer evolutions below ice covers as reported by McPhee* (1975) or Farmer (loc.cit.) are of particular interest in this context.

10.6 Explicit simulation of time-dependent developments

The actual evolution of mixed layers and surface temperatures with time depends on the vagaries of the wind, air temperature, radiation and so forth.

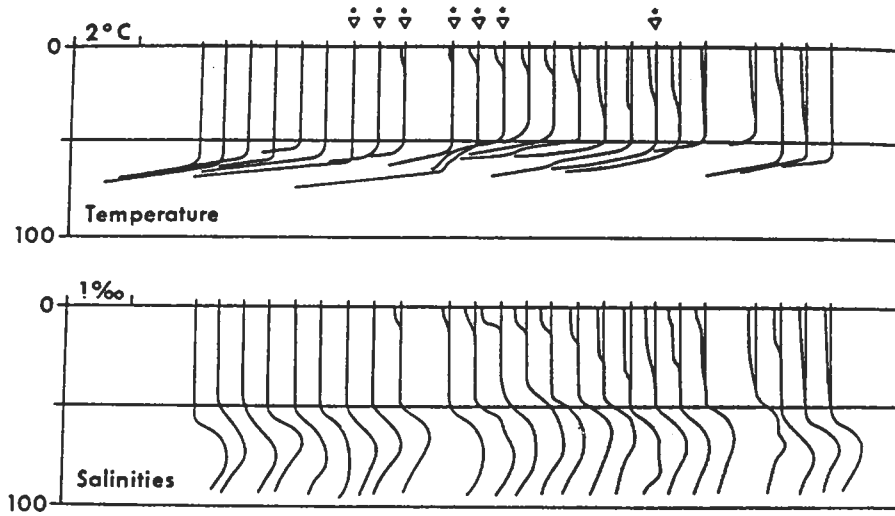


Fig. 10.3 - Downward mixing of a fresh water lens after showers, based on hourly sounding at about 5°N, 21°W in July 1972. Showers are marked by the conventional international symbol. Note the characteristic salinity maximum below the mixed layer base. The figure has been kindly supplied by F. Ostapoff. (See also Ostapoff, Tarbeyev and Worthem, 1973).

In other words, $u_* \approx u_*(t)$ and the same applies to other forcing processes. The rate of layer deepening depends in addition on the stratification in the water below. Two special cases which have drawn particular attention are the deepening of a mixed layer following the sudden onset of a storm and the simulation of diurnal or annual cycles.

a. The deepening of a wind-stirred layer

A study of layer deepening as a function of time shows how the different processes and equilibria, which were discussed in Section 10.4, necessarily dominate the development. An orderly time sequence of separate physical regimes becomes apparent. This separation allows us in principle to evaluate the free model parameters (m, n, s) independently from different time segments of a single record.

Following Niiler (1975) and de Szoeke* and Rhines (1976) we shall consider a highly simplified model, which is characterized initially by a fluid at rest with a surface buoyancy b_0 and buoyancy gradient

$$\frac{\partial b}{\partial z} = N^2 = \text{constant.} \tag{10.47}$$

At a time $t=0$ a constant stress ρu_*^2 and a constant cooling rate B_0 are applied to the surface. The penetration of solar radiation is neglected ($\gamma = \infty$).

The assumptions of a constant N and constant forcing after the initial

impulse represent a highly idealized state. Real oceanic conditions are never quite as simple. For example, B_0 cannot remain constant, in general, when the temperature of the deepening layer changes. In spite of its artificiality - or perhaps because of it - the simplistic model with its constant forcing and uniform initial lapse rate reveals rather clearly the succession of different regimes.

Following the beginning of the stirring process at $t=0$, a mixed layer with constant buoyancy \bar{b} is established. This leads to the establishment of a density discontinuity at the bottom of the layer

$$\Delta b = \bar{b} - b_h = \bar{b} - b_0 + hN^2. \tag{10.48}$$

The value of b_h - the original buoyancy at the level h - is obtained from the integral of Eq. (10.47). The mixed layer buoyancy must be equal to the mean of the buoyancy which existed in the layer between $z=0$ and $z=h$ before mixing, minus the time integral of the surface buoyancy flux B_0 . With B_0 assumed constant, one gets:

$$h\bar{b} = \frac{h}{2} (b_0 + b_h) - B_0 t.$$

Elimination of \bar{b} between the last two equations yields:

$$c_i^2 = \Delta bh = \frac{1}{2} N^2 h^2 - B_0 t. \tag{10.49}$$

We introduce Eqs. (10.40) and (10.49) into the turbulence energy equation (10.29) with $I_0=0$, $B_0 \geq 0$ and with $C|\bar{v}| \ll \rho w_e$. This equation then assumes the form

$$\frac{1}{2} \frac{dh}{dt} [q^2 + \frac{1}{2} h^2 N^2 - B_0 t - 2su_*^4 f^{-2} h^{-2} (1 - \cos ft)] = \mu u_*^3 + \frac{1}{2} B_0 h. \tag{10.29'}$$

A B B' C D E

For a scale analysis, the magnitude of the external parameters has to be specified. We shall use typical mid-latitude values of $u_* = 1.5 \text{ cm s}^{-1}$ (corresponding to a fresh breeze with a velocity of about 12 m s^{-1}), $B_0 = 2 \times 10^{-3} \text{ cm}^2 \text{ s}^{-3}$ (corresponding to a surface heat loss of $0.01 \text{ cal cm}^{-2} \text{ s}^{-1}$), $N^2 = 2 \times 10^{-4} \text{ s}^{-2}$ and $f = 10^{-4} \text{ s}^{-1}$.

Immediately after the onset of the stress, when h and t are both small, term (D) can be balanced only by term (A). At this stage the mixed layer is of the same order or smaller than the depth of the constant stress layer and therefore $q^2 = u_*^2$. Integration of Eq. (10.29'), with only terms (A) and (D) different from zero, yields

$$h = 2\mu u_* t. \tag{10.50}$$

The depth grows linearly with time at this state. This regime must continue until term (B) becomes comparable to (A). This happens when the layer depth has reached a value h_1 at which $u_*^2 = c_i^2$. To compute h_1 , we introduce the value of c_i^2 from Eq. (10.49) into this equality and substitute for t from Eq. (10.50).

This yields

$$h_1 = \frac{u_*}{N} \left[\sqrt{2} + \frac{B_0}{2mNu_*^2} + \sqrt{2} \left(\frac{B_0}{2mNu_*^2} \right)^2 + \dots \right] \approx \frac{u_*}{N} \sqrt{2}. \quad (10.51)$$

The last approximation is a consequence of the chosen numerical values of B_0 , N and u_* , with $m=1$. With these numerical values, the depth h_1 is only about 1.5 meters, which shows that the mixed layer depth is indeed comparable to the depth of the quasi-constant stress layer during the validity of this regime. The layer reaches the depth h_1 within a time

$$t_1 = \frac{h_1}{2mu_*} = \frac{1}{\sqrt{2}mN}; \quad (10.52)$$

assuming $m=1.25$ at this state, one finds that t_1 is only about 40 seconds.

In laboratory experiments where N is usually larger than in nature the development proceeds even faster. For $t > t_1$ the first term in Eq. (10.29') becomes negligibly small and this justifies the omission of this term in the discussions presented in Section 10.4.

At the time t_1 the term (B) in Eq. (10.29') is large compared to (B').

By expanding $\cos(ft)$ it can be shown readily that it is also larger than (C) which becomes important only after a significant fraction of one inertial period has passed. Until that happens there must be a balance between terms (B) and (D), which makes the ratio of dh/dt to u_* proportional to the inverse Richardson number $(u_*/c_1)^2$. Integration of Eq. (10.29') with all terms except (B) and (D) negligible yields:

$$h = \frac{u_*}{N} (12mNt)^{1/3}. \quad (10.53)$$

The layer deepens now at a rate which is proportional to the cube root of t .

This cube root regime continues to prevail until either (C) or (E) becomes relatively large. With the chosen numerical values of f and B_0 the former will occur first. Terms (B) and (C) become about equal when the layer has expanded to a depth

$$h_2 \approx \frac{u_*}{N} (6ms^{-1/2}). \quad (10.54)$$

This occurs at a time

$$t_2 \approx \frac{1}{N} (18m^2 s^{-3/2}). \quad (10.55)$$

It is interesting to note that the transition time t_2 is independent of u_* or f .

Gradually the mean flow, or inertial motion, accelerates to make term (C) comparable to term (B). The sum in brackets then becomes very small. To achieve balance with the energy input from the wind, dh/dt has to become very large, at least during some interval in this regime. In other words, we should

expect a very rapid deepening of the mixed layer when the inertial current velocity is of the same order as the internal wave velocity C_1 . Exceptionally rapid deepening in such circumstances has indeed been observed by Price*, et al. (1976) in the Gulf of Mexico.

The term (C) reaches its largest value after one-half pendulum day, that is, at a time

$$t_3 = \pi/f. \quad (10.56)$$

If we accept the arguments which were put forth by Pollard, et al. (1973), the corresponding mixed layer depth can be computed by substituting Eqs. (10.49) and (10.56) into Eq. (10.41). This yields:

$$h_3 = \frac{u_*}{N} (2N/f)^{1/2} s^{1/4}. \quad (10.57)$$

For $t > t_3$ the value of the term (C) becomes smaller again and the regime corresponds then to the condition discussed in Section 10.4e. There will be a renewed balance between terms (B) and (D) and continuing deepening with the cube root of time until the layer depth exceeds the value of

$$h_4 = \frac{m}{n} L_* = \frac{2mu_*^2}{nB_0}. \quad (10.58)$$

Further deepening beyond h_4 would be described by an equation of the form

$$\frac{dh}{dt} (N^2 h^2 - B_0 t) = 2nB_0 h. \quad (10.59)$$

At this depth, however, the assumption of a constant N becomes very unrealistic indeed.

The successive dominance of different regimes is summarized in Table 10.1.

TABLE 10.1

Range of transitional regimes in a deepening wind-stirred layer (the computation of particular transition depths and times is based on the following specified values of the external and internal parameters: $u_* = 1.5 \text{ cm s}^{-1}$, $B_0 = 2 \times 10^{-3} \text{ cm}^2 \text{ s}^{-3}$, $N = 1.4 \times 10^{-2} \text{ s}^{-1}$, $f = 10^{-4} \text{ s}^{-1}$, $m = 1.25$, $s = 0.7$, $n = 0.7$, $C = 0$.)

Transition Time	Transition Depth	Regime
0	0	{ linear growth of h
$N^{-1}(\sqrt{2}m)^{-1}$ (40 sec)	$\frac{u_*}{N}\sqrt{2}$ (1.5 cm)	{ $h = \tau^{1/3}$
$N^{-1}(18m^2s^{-3/2})$ (1 hour)	$\frac{u_*}{N}(6ms^{-1/2})$ (10 m)	{ inertial deepening
f^{-1} (9 hours)	$\frac{u_*}{N}(2N/f)^{1/2}s^{1/4}$ (17 m)	{ $h = \tau^{1/3}$
$N^{-1} \frac{2}{3} m^2 \left(\frac{u_*^2 N}{nB_0} \right)^{-1}$ (10 days)	$\frac{2mu_*^2}{nB_0}$	{ deep convective erosion

It should be noted that different values of the forcing parameters and initial conditions would lead to different transition times and depths. In the present model, the choice of a relatively small value for B_0 allowed us to ignore the term (B') in Eq. (10.29') through most of the development. This will not always be the case. The internal wave radiation, which has been neglected in our computation ($C=0$), must have some influence particularly on the development of the inertial regime. Values of C could be derived possibly from observations of the phase and amplitude of the inertial oscillations. They cannot be derived directly from the present model. Lastly, the chosen value of m is that based on the old Kato-Phillips experiments. The choice of a larger, variable m would have stretched out the validity of the second and fourth regimes in both time and depth.

b. Cyclical changes

In studies of the diurnal and seasonal mixed layer evolution, the forcing functions B_0 and u_* cannot be constant; in fact, the former in particular has necessarily a cyclical component. It is also inappropriate now to stipulate, a priori, the density structure of the water column below the mixed layer. Instead, modellers have assumed usually that this structure was established during the spring heating season, when the mixed layer reached down to the relevant depth. As the heating increases, the layer becomes shallower as indicated by the Eqs. (10.32) or (10.36) leaving a stably stratified fluid below. During this process, the layer is decoupled from the lower water, which remains more or less undisturbed, at the temperature which it had when it was last directly in contact with the surface. The corresponding density structure is conserved until it is again swallowed up by the deepening mixed layer in the cooling season.

In the real ocean, conditions at depths below the mixed layer can obviously not be exactly conserved. Diffusion tends to smooth out gradient changes. More important even is the fact that the seasonal development is not a smooth process, but one which is punctuated by storms which can mix surface water down to considerable depths within a relatively short time. However, this process can be included in models and if it is allowed for, the stipulated conservation of conditions at depths below the mixed layer is in fact reproduced, at least qualitatively, over many parts of the ocean. In general, the analysis has to be carried out numerically unless one stipulates a very special form of the surface heating B_0 as a function of time. Obviously, if

the ocean below the layer "remembers" how its temperature structure was established, the computer has to do the same. In other words, numbers for the temperature distribution which had been established by the receding mixed layer during the heating season, have to be stored in memory until the deepening layer reaches again down to the same levels. The process has been simulated in laboratory experiments (Turner and Kraus, 1967).

It is characteristic for the cyclical changes that the evolution of the surface temperature is not in phase with the layer depth. This fact is well simulated by the mixed layer models. For example, Eq. (10.36) shows that during surface heating ($B_0 < 0$) the layer depth reaches its smallest value when the heating $|B_0|$ reaches its maximum - that is at the time of the summer solstice for the seasonal case, or at noon for the diurnal evolution. At that time $w_e = dh/dt = 0$, but from Eq. (10.22) it can be seen that then $dT_0/dt \neq 0$;

in fact, the surface temperature rise will tend to be largest at that time.

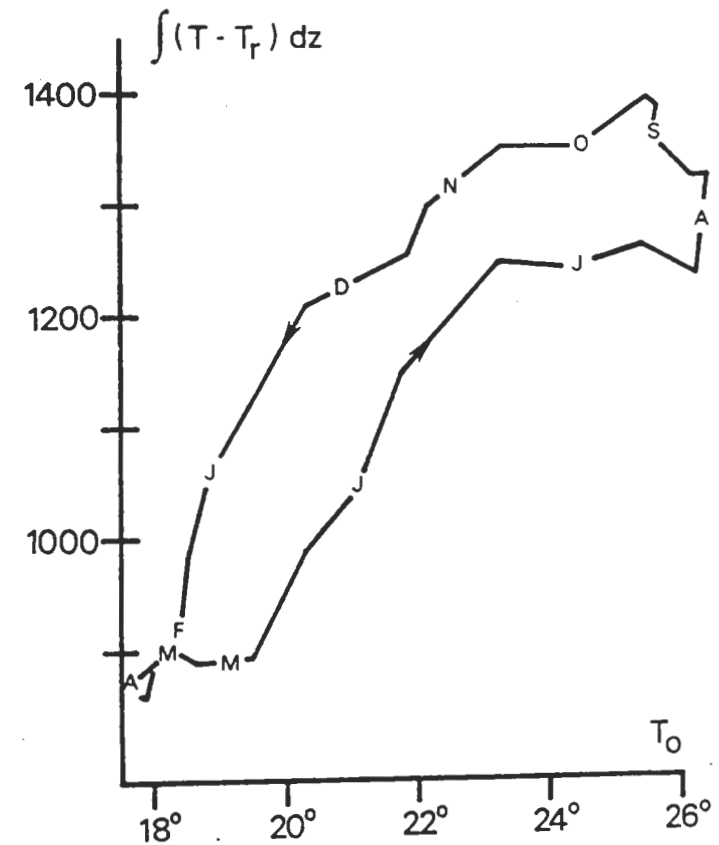


Fig. 10.4 - Heat content as a function of surface temperature at Ocean Weather Station Echo (35°N, 48°W). The integral extends from a fixed depth of 250 m to the surface. The reference temperature T_r represents the mean of the temperature at 250 m and 275 m depth. (After Gill and Turner, 1976).

This out-of-phase relationship of T_0 and h has been noted in many series of lake and ocean observations (see Kraus (1972) for diagrams and references). Because of it, any plot of h against T_0 or B_0 as a function of time will exhibit a hysteresis loop. Instead of plotting h against T_0 directly, one can plot the total heat content (or the corresponding mass deficit) of a water column in the upper ocean against the surface temperature. Such a plot is shown in Fig. 10.4 which is drawn from Gill and Turner (1976) and is based on data from ocean station Echo (35°N, 48°W). It can be seen, for example, that the surface temperature is much higher in August than in November, but the mixed layer is shallower in summer and the heat content of the water column in the two months is about the same. The existence of this hysteresis loop

is, of course, simply a manifestation of the ocean's capacity to store heat beyond the heating season. As such, it has an influence on the climate, and indeed the livability of the planet, which cannot be overestimated. (See also Holland, Figs. 2.6 and 2.15 for computer simulation of hysteresis loops.)

As mentioned above, the original models with forcing by a cyclical B_0 did not produce a completely cyclical response. Without suitable parametrization of the dissipation, the convective layer becomes deeper and the potential energy increases from cycle to cycle. This is due to the continuing positive energy input by the wind ($u_*^2 > 0$). To model real cyclical developments one has to let m and n both go to zero as the layer becomes deep. All the input energy is then dissipated and none is available to increase the potential energy of the water column excessively. Alternatively one can allow for a general slow upwelling w . Such a widespread upwelling is indeed needed over much of the oceans, to compensate for the production of bottom water by sinking in high latitudes.

10.7 Concluding remarks

One-dimensional mixed layer models may well become useful components in more comprehensive ocean, climate and biological models. They have the advantage of being relatively simple and of providing a rather direct physical insight. They can yield reasonably realistic simulation of diurnal and of seasonal temperature changes in lakes and in suitable chosen ocean areas where horizontal advection is insignificant. The realism is improved if one chooses some functional form for the factors m and n which causes them to go towards zero as the layer becomes very deep. A zero value of these factors implies a balance between turbulence generation and dissipation. It does not imply an invariant layer depth, though it must cause the disappearance of the discontinuity at the layer base.

The ability of the simple mixed layer model to simulate rapid changes after storms is more questionable. They seem to work sometimes, but at other times they do not simulate the actually observed oceanic development very well. This may be due partly to the dependence of the development on the exact character of the dissipation and also to the fact that horizontal variations may not be negligible in these circumstances.

We wish to thank once more all the contributors to the Urbino working group on one-dimensional modelling. In preparing this report, we had the advantage of support from the National Science Foundation under Grant No. NSF GA 33550X and from the Office of Naval Research, Grant No. N0014-75-C-0299, NR083-315.

Chapter 10a NOTE ON THE ROLE OF INTERNAL WAVES IN THERMOCLINE EROSION

L. H. Kantha

In the preceding chapter by Niiler and Kraus, (referred to below as N&K), the influence of internal waves on entrainment processes has been essentially ignored. There is reason to suspect, however, that their influence could be quite substantial, at least under some conditions. It is the purpose of this note to discuss the possible effect of internal waves on the entrainment rate and on the associated energy flux.

Internal waves can be generated locally by turbulence or externally by a distant storm. Waves always radiate energy away from the area where they are being generated. They can cause thus a local energy loss from the mixed layer in the area below a storm. This tends to reduce entrainment, simply because less energy is available for the lifting of the dense lower fluid into the mixed layer. On the other hand, waves which propagate into the region can make additional energy available, which might increase the rate of layer deepening.

The energy radiated away by locally generated waves was parameterized in the Eqs. (10.26) and (10.27) of N&K in the form $E_i/\rho \approx c|\bar{v}|^3$ and lumped together with the shear production of turbulence kinetic energy at the bottom of the mixed layer. The term was subsequently dropped. However, in any case, this parameterization is rather arbitrary. The energy supplied to the waves must depend upon the amplitude and the length scale of the interface perturbations and upon the stratification in the fluid below. If the region below the interface is not stratified, internal waves propagating into the interior cannot be generated. It follows that the energy loss might be expressed more appropriately in the form:

$$\frac{E_i}{\rho} \approx \frac{E_i}{\rho} (q_z, l_m, N, \Delta b),$$

with q_z the root mean square vertical component of the turbulent velocity, l_m the integral length scale of turbulence within the mixed layer; N is the buoyancy frequency in the fluid below and Δb has the same meaning as in N&K. Using dimensional analysis:

$$\frac{E_i}{\rho q_z^3} = g \left(\frac{\Delta b h}{q_z^2}, \frac{N q_z}{\Delta b}, \frac{l_m}{h} \right). \quad (10a.1)$$

For brevity's sake we write $N q_z / \Delta b = \delta$. With the interface treated as a sharp discontinuity $\Delta b h = c_f^2$; and with the integral scale length proportional to the layer depth in fully developed mixed layer turbulence $l_m \propto h$, this allows Eq. (10a.1) to be rewritten in the form:

$$\frac{E_i}{\rho q_z^3} = g_1 \left(\frac{c_f}{q_z}, \delta \right). \quad (10a.2)$$